2018

Application of Ground-Penetrating Radar in measuring Corn seeds (CS) Spacing and Planting depth in different soils

Kenneth O. M. Mapoka
Iowa State University, komapoka@iastate.edu

Stuart J. Birrell
Iowa State University, sbirrell@iastate.edu

David J. Eisenmann
Iowa State University, djeisen@iastate.edu

Application of Ground-Penetrating Radar in measuring Corn seeds (CS) Spacing and Planting depth in different soils

Abstract
The effects of seed spacing and depth at planting contribute greatly to corn production. Correct seed spacing, and planting depth may enable moisture absorption which facilitates seedling emergence with the establishment of healthy and robust root structure. Therefore, measuring seed spacing and planting depths in a closed furrow is necessary for precision seeding and corn production. In agricultural applications, Ground Penetrating Radar (GPR) is used for nondestructive evaluations as a potential sensor to maximize the qualitative and precision or repeatable assessments in long-term research. Yet GPR system has not been used to measure seed spacing and planting depths, but it has the potential to measure the two parameters. The objective of this experimental research was to use a non-destructive 2.6 GHz GPR system to detect agricultural Corn Seeds (CS) buried at different depths (3.81, 6.35, and 8.89 cm) and spacing (15.24 and 25.4 cm) in sandy-loam and loam soils. The data was processed using the Fast Discrete Curvelet Transform to denoise and enhance edge responses from CS. In bone-dry soils some CS were detected, while in intermediate and moist soils it was difficult to detect CS. The two-way travel time in nanoseconds and soil dielectric permittivity from experimental data were used to estimate planting depth while the spatial distance between the CS was computed from the antenna cart encoder. The Topp's dielectric, soil mixing, and the Topp-Mixing (TM) model were used to estimate the soil dielectric permittivity. The TM model was developed as a function of the Topp's dielectric, and soil mixing models to minimize and optimize planting depth error (PDE). The TM model was found to be effective in predicting permittivity used to approximate planting depth with minimal PDE. The assessment of the 2.6 GHz antenna effectiveness was based on the percent coefficient of precision (CP3) and coefficient of planting depth accuracy (CPDA). The CP3 values were < 30% but differed for the three moisture groups and soil types. The TM model had the best CPDA of 9.9%. While the results are promising, more research is needed to enable detection and depth measurements of CS in soil conditions that are typical of a ploughed field.

Keywords
Corn seeds, CPDA, GPR, Planting Depth, Topp-Mixing, Dielectric permittivity

Disciplines
Agriculture | Agronomy and Crop Sciences | Bioresource and Agricultural Engineering

Comments
This proceeding is published as Mapoka, Kenneth OM, Stuart J. Birrell, and David J. Eisenmann. "Application of Ground-Penetrating Radar in measuring Corn seeds (CS) Spacing and Planting depth in different soils." 2018 ASABE Annual International Meeting, Detroit, MI, July 29-August 1, 2018. Paper no. 1801351. DOI: 10.13031/aim.201801351. Posted with permission.

2950 Niles Road, St. Joseph, MI 49085-9659, USA
269.429.0300 fax 269.429.3852 hq@asabe.org www.asabe.org

An ASABE Meeting Presentation
DOI: https://doi.org/10.13031/aim.201801351
Paper Number: 1801351

Application of Ground-Penetrating Radar in measuring Corn seeds (CS) Spacing and Planting depth in different soils

Kenneth O. M. Mapoka[a], Stuart J. Birrell[a], David J. Eisenmann[b]
[a]Agricultural and Biosystems Engineering, Elings Hall, Iowa State University and [b]Center for Nondestructive Evaluation, Applied Science Complex II, Iowa State University.

Written for presentation at the
2018 ASABE Annual International Meeting
Sponsored by ASABE
Detroit, Michigan
July 29-August 1, 2018

ABSTRACT. ***The effects of seed spacing and depth at planting contribute greatly to corn production. Correct seed spacing, and planting depth may enable moisture absorption which facilitates seedling emergence with the establishment of healthy and robust root structure. Therefore, measuring seed spacing and planting depths in a closed furrow is necessary for precision seeding and corn production. In agricultural applications, Ground Penetrating Radar (GPR) is used for nondestructive evaluations as a potential sensor to maximize the qualitative and precision or repeatable assessments in long-term research. Yet GPR system has not been used to measure seed spacing and planting depths, but it has the potential to measure the two parameters. The objective of this experimental research was to use a non-destructive 2.6 GHz GPR system to detect agricultural Corn Seeds (CS) buried at different depths (3.81, 6.35, and 8.89 cm) and spacing (15.24 and 25.4 cm) in sandy-loam and loam soils. The data was processed using the Fast Discrete Curvelet Transform to denoise and enhance edge responses from CS. In bone-dry soils some CS were detected, while in intermediate and moist soils it was difficult to detect CS. The two-way travel time in nanoseconds and soil dielectric permittivity from experimental data were used to estimate planting depth while the spatial distance between the CS was computed from the antenna cart encoder. The Topp's dielectric, soil mixing, and the Topp-Mixing (TM) model were used to estimate the soil dielectric permittivity. The TM model was developed as a function of the Topp's dielectric, and soil mixing models to minimize and optimize planting depth error (PDE). The TM model was found to be effective in predicting permittivity used to approximate planting depth with minimal PDE. The assessment of the 2.6 GHz antenna effectiveness was based on the percent coefficient of precision (CP3) and coefficient of planting depth accuracy (CPDA). The CP3 values were < 30% but differed for the three moisture groups and soil types. The TM model had the best CPDA of 9.9%. While the results are promising, more research is needed to enable detection and depth measurements of CS in soil conditions that are typical of a ploughed field.***

Keywords. Corn seeds, CPDA, GPR, Planting Depth, Topp-Mixing, Dielectric permittivity

Introduction

The effects of Corn Seeds CS spacing and depth at planting significantly influence to corn yield potential. CS can be planted at depths ranging from 3.81 to 8.89 cm and spaced 13.96 to 25.40 cm depending on the soil abiotic factors (particularly soil moisture content, and texture), variety and soil water holding capacity. Correct CS spacing, and planting depth may enable moisture absorption which facilitates seedling emergence with the establishment of healthy and robust root structure. Literature highlights the critical effects of these two parameters at planting for corn production (Beck, 2014; Doerge et al., 2015; Hussen et al., 2013). Beck, (2014) conducted in-situ experimentation with several planting depths; the results were variable with high losses at shallow and deep depths, while those CS planted in the recommended theoretical planting depths yielded low losses. In another study, Liu et al., (2004) emphasized the fact that corn was more responsive to the emergence variability rather than in-row spacing variability. The study also indicated that corn emergence variability reduced the total yield while the in-row spacing did not have an effect on the yield. However, agronomists and producers agree that uniform in-row spacing and depth control at planting provide the highest probability to achieve the maximum yield potential (Andrade & Abbate, 2005). The importance of plant spacing and depth is reflected in the development and publications of the ISO Standard 7256/1, developed to assess the performance of precision planters, i.e., measuring actual seed spacing and determining the uniformity of trench depth and seed depth in the soil (Koller et al., 2014).

Dielectric properties refer to inherent constitutive characteristics of a material which govern the electromagnetic behavior of the propagated wave through a material. CS are dielectric composites that have no free moving charges within their cellular membrane. It is well known that water molecules influence dielectric properties; therefore, for any material that possesses any amount of water, a range of dielectric constants can be exploited. The latter applies to CS, where, at storage, their moisture ranges from 5% to 14%. This moisture limit creates an environment whereby microwave frequencies can be used to determine CS moisture noninvasively without compromising the grain quality (Nelson, 2005).

No efforts have been presented in the literature to the effect of measuring corn planting depth and spacing using state-of-the-art methods. This research work focusses on quantitatively measuring CS planting depth and spacing using non-destructive Ground Penetrating Radar (GPR) technique. The GPR operates by sounding and receiving electromagnetic (EM) energy from the ground as well as embedded targets. The transmittance, reflectance, and absorbance of the EM energy are governed by the antenna center frequency and the electromagnetic properties of the medium under test. The dielectric component of the CS may play a significant part in the detection. GPR EM waves are in the microwave frequency range. Therefore, it can be used to map the dielectric CS. In numerous GPR studies or surveys, the dielectric features of agricultural materials are frequently the response variables; however, targets of that nature (dielectric) are not good reflectors. Their size and orientation in the soil may be a factor significantly affecting their detectability using the GPR.

The GPR has been successfully used in many sensing applications in agriculture and forestry (Barton & Montagu, 2004; Butnor et al., 2003; Butnor et al., 2001; Cui et al., 2013; Dannoura et al., 2008; Raper et al., 1990). A simulation study was performed by Mapoka et al., (2016) to evaluate the possibility of using GPR to map synthetic (metal having same dimensions as CS) and CS. The GPR model of antenna frequencies of 1.6 and 2.6 GHz successfully detected the modeled synthetic CS as well as CS having approximately the same dielectric properties as the real seed, with substantial response amplitudes except in conditions where the soil models had higher clay content and bulk density.

GPR waves are sensitive to abrupt changes of the material constitutive (electrical properties) conditions, which leads to inevitable multiple intermittent scattering within the subsurface (non-uniformity reflectance from soils with shallowly buried targets). The GPR images convey the positions of the buried targets in terms of hyperbolic responses; therefore, a high attenuation medium or multiple intermittent reflections may significantly reduce GPR image and target responses quality, which may negatively impact the data analysis and interpretation. In this research, the overall performance of the GPR was assessed by the measured temporal spacing and depth of the buried CS.

The capability of measuring planting depth using the GPR may have an essential contribution in precision farming to maximize corn production. Therefore, the primary goal of this investigation was to use a 2.6 GHz GPR antenna to map CS at different planting depths and spacing buried in different soils and conditions. The specific objectives of this research work were to (1) evaluate the GPR antenna on sandy-loam, and loam soils at three soil volumetric moisture content groups with CS buried at three different planting depths, and two different spacing and, (2) quantify corn seed planting depths and spacing.

Materials and methods

Experimental Conditions

The experiment was conducted under controlled laboratory conditions. Two natural sandy-loam and loam soils were used in the investigation. The sandy-loam was collected from the Applied Science Iowa State University farm (Moore), Ames, Iowa. The loam soil was collected from Iowa State Farm, in Boone County, Iowa (Latitude 42.021196 N, Longitude 93.773627 W), with which the soil series in the farm were the clarion (66.11 ac), Canisteo (35.76 ac), and Nicollet (31.63 ac) (Andrews, 1981).The soils were collected from depth range of 0 to 40 cm.

Prior to conducting experiments, collected soils were processed: the sandy-loam and loam soils were sieved using a sieve size of 5 mm and allowed to air-dry to lower soil volumetric moisture content (VMC). The purpose of sieving the soils was to reduce plant residues, eliminate clods and rocks, and other resistive sediments, which may otherwise hinder corn seed detection. Moreover, due to the lack of sandy soil in Iowa, Boone County region, the sandy-loam soil collected was selected to have low clay content and high percent of the sand component. The sandy-loam soil texture consisted of 67% sand, 25% silt, and 8% clay; the loam had 49% sand, 34% silt, and 17% clay. Accordingly, the sandy-loam and loam soils were classified as non-saline due to low electrical conductivity values of 0.179 dS m^{-1} and 0.505 dS m^{-1}, respectively (Test, 1998). The assumption was that the two soils represent the average soil characteristics where they were collected with less organic matter and undulated soils. The sandy-loam and loam organic matter measured were 2.64% and 4.74%, respectively. The soil bulk density were measured according to the ASTM D7263 and ASTM D2216 standards (ASTM, 1972, 2018); thereby, determining that the dry bulk density of sandy-loam and loam were 1.41 g cm^{-3} and 1.47 g cm^{-3}. The soils information is presented in table 1. The two soils were transferred into the soil containers (soil-bins) measuring $152.4\ long \times 29.21\ wide \times 25.40\ deep$ cm. Figure 1 represents the experimental layout of soils in the bin and seeds placed at different depths and spacing. The soil bins were filled with soils to a depth of 20.32 cm.

Table 1. Soil information used in the study.

Textural class	Sand (%)	Silt (%)	Clay (%)	Bulk density (g cm^{-3})	Salinity (dS m^{-1})	Organic matter (%)
Loam	49	34	17	1.47	0.505	4.47
Sandy-loam	67	25	8	1.41	0.179	2.64

Corn Seeds

The Corn Seeds (CS) variety used was the Pioneer P0339AMXT with a Precision Design Rounds (PDR) seed size (1459 kernels/lb.) The CS moisture content was determined by oven drying at 135C for 2 hours (AOAC 930.15). The average measured CS moisture content was 10.05%, at the time the GPR experiments were conducted. The physical dimensions (*Length, Width, and Height*) of the 30 CS (sample size) were measured using a Vernier caliper of accuracy of 0.1 cm. The average dimensions were 1.15 cm, 0.73 cm, and 0.55 cm, with standard deviation of 0.06 cm, 0.03 cm, and 0.05 cm, respectively. A total of six CS were buried in a row at planting depths of 3.81 cm (1.5 in), 6.35 cm (2.5 in), and 8.89 cm (3.5 in). The first three CS were spaced every 25.4 cm (10 in), equivalent to a corn population of 21000 plants per acre at 76.2 cm row spacing. The last three in the row spaced every 15.24 cm (6 in), equivalent to a corn population of 35000 plants per acre at 76.2 cm row spacing, respectively (Figure 1a). The CS were buried in sandy-loam and loam soils (Figure 1b). The seed orientation did not matter because of their small size.

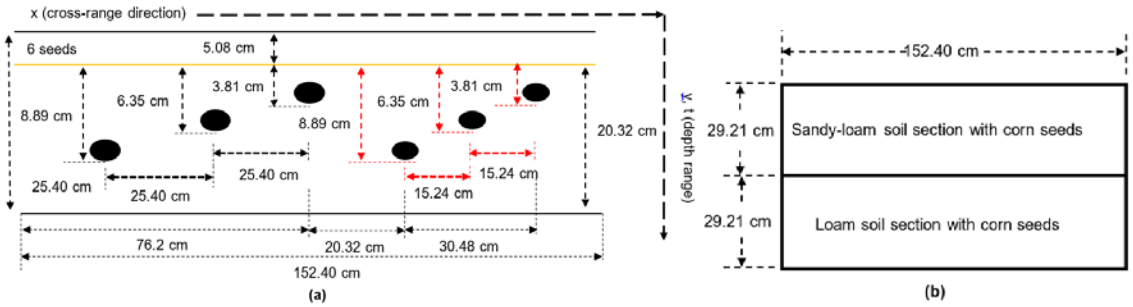

Figure 1. Experimental setup (a) CS inside soil box section where seeds were buried at different planting depths and spacing in a single row, (b) top view of a single soil type in a box section.

Subsoil inclusions (i.e. soil water, saline concentration, texture and other unconsolidated and consolidated particles) can be extremely difficult to distinguish from other dielectric targets, due to the fact that soils are dielectric with varying constituents. Prior to using actual CS, a higher contrasting steel dielectric targets (i.e. conductive) were used to show how the hyperbolic responses would appear in a B-scan at different depths (figure 2). These steel targets having the same dimensions as the CS and were placed at the exact depths as the CS. Figure 2 shows the hyperbolic trend at the local position of each transect. Therefore, in case of CS, the hyperbolic response patterns would be expected to mimic the depiction in figure 2. However, the dielectric properties of the steel and that of the CS are markedly different; accordingly, the hyperbolic responses from CS will be less distinct and lower intensity when compared to figure 2.

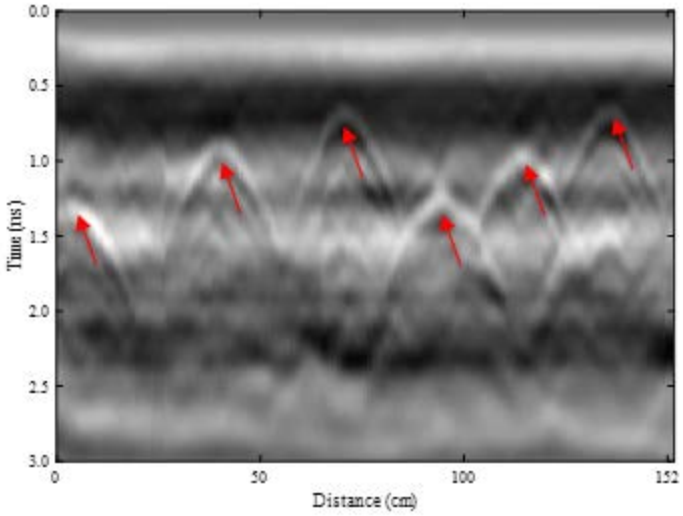

Figure 2. Raw B-scan of steel targets at the exact location of the CS in sandy-loam soil. The red arrows show the exact positions of the steel targets

Ground Penetrating Radar (GPR)

The experimental data used in this investigative research was collected using a portable Subsurface Interface Radar (SIR) 3000 GPR from Geophysical Survey Systems, Inc. with an antenna frequency of 2.6 GHz (model 52600, GSSI). The 2.6 GHz antenna transmit short electromagnetic wave pulses into proximal soil surface and receive reflections from atop soil, within the soil, and buried reflectors. The scattering in the soil is primarily governed by the dielectric discontinuities. The data collected at the receiver (reflected GPR waves) consists of the air-soil response amplitude (electric field strength, V m^{-1}), time of flight (ns), and CS response amplitude dependent upon soil and CS properties. That is referred to as an A-scan in GPR technical terms whereby the time of flight would be on the abscissa (x axis) to signify the depth, and the response amplitude magnitude on the ordinate (y axis). The B-scan (fig. 2) is created by stitching together a series of multiple A-scans collected from the ground of predetermined spatial distance and scanned at fixed sampling time intervals. The spatial distance (cm) is on the abscissa and total time (ns) on the ordinate. The most important feature of the GPR is the resolution and it is application specific (i.e. assessed depths, material under test). The GPR antenna has two classes of resolution, namely the vertical and horizontal resolution (Pérez-Gracia et al., 2008; Rial et al., 2009). The vertical and horizontal resolutions are defined in equation (1) and (2), respectively.

$$T_m = \frac{c}{4 * f\sqrt{\varepsilon}} \quad [1]$$

$$A = \frac{\lambda}{4} + \frac{D}{\sqrt{(\varepsilon + 1)}} \quad [2]$$

where T_m – minimum thickness resolved (cm), c – the speed of light (cm/s), f – antenna frequency (GHz), ε – relative dielectric permittivity, A – radius of the footprint (cm), λ – antenna frequency wavelength (cm), and D – depth (cm). These two antenna resolution defines the ability of the GPR to image and display finer details of an object in a discernible way.

Data collection

The laboratory experiments were arranged in a completely randomized design. The main treatment in the soil bins were the two soil types, three soil VMC groups, two CS spacing, and three CS depths, and the Pioneer P0339AMXT variety of CS as the response variable ($2 \times 3 \times 3 \times 2 = 36$ combinations). Non-saline sandy-loam and loam soils were used, and the CS were buried as shown in figure 1a. Five replicates for each of these treatments were collected using the 2.6 GHz GPR antenna. A total of 180 experimental test runs $5\ replications \times 36$ combinations $= 180$ runs) were performed using 1080 CS ($180\ runs \times 6\ CS = 1080\ CS$) (1079 spacing), nominally. The CS were used once and discarded after each test. Radargrams of the five replicates were collected along a row from the widely spaced CS of 25.4 cm (10 in) to a much narrower spacing of 15.24 cm (6 in) as shown in Figure 1a. The 2.6 GHz antenna was mounted on a cart which had an encoder to measure accurately spatial distance or position. The cart rail was designed to be placed atop soil to prevent the cartwheels from plowing into the soils, hence causing drag. Moreover, system control parameters were adjusted to suit a soil type in the soil bins. The system control settings for the SIR-3000 unit are presented in table 2. The VMC measurements were divided into three groups, *dry*, *intermediate*, and *moist* soil (table 3). The soil VMCs were measured in three separate occasions with an interval of twenty days between VMC groups. In addition, the VMCs corresponding to the five replicates were measured using the oven dry method as per the ASTM D2216 standards.

Table 2. System control parameters for the SIR-3000 unit

Parameter description	
Antenna model	52600
Samples per scan	1024
Scans per foot	100
Scans	60
Bits per sample	16
Number of gains	7

Table 3. Classification of soil VMC groups

VMC group	VMC (%)
Dry	0 < VMC < 5
Intermediate	5 > VMC < 13
Moist	13 > VMC < 20

Two variables: *the seed spacing and planting depth*, were measured to determine the efficacy, consistency, and accuracy of the GPR in mapping CS buried in sandy-loam and loam soils, at different soil VMCs. The investigation was conducted in three VMC groups: *dry, intermediate, and moist*. The dry class had VMCs ranging from 2.31% to 2.95% for the sandy-loam and 2.47% to 2.96% for the loam. The intermediate class the VMCs were determined to be between 10.37% to 11.34% for the sandy-loam and 10.22% to 13.28% for the loam, and lastly, the moist class ranged from 15.03% to 17.07% for the sandy-loam and 16.03% to 18.80% for the loam soils. The parameters in table 2 were kept constant for the entire data collection; however, the calibrated wave velocity or total wave time to traverse the soil was variable according to *in-situ* soil bin conditions. On the other hand, the seven antenna gains were variable depending on soil type and VMC group. For instance, for a soil type and VMC group the gain points were kept constant; however, migrating to a different experimental unit the gains were changed accordingly to suit soil bin conditions. The antenna gains were calibrated at seven points, where their breakpoints were time-varying with respect to depth in the soil bin.

Application of image processing for discrimination of CS responses

GPR data is highly susceptible to noise resulting from internal soil inhomogeneities (varying contrasting constitutive properties as influenced by soil moisture contents, composition, and bulk density). The contrasting constitutive properties may cause multiple absorption and intermittent reflections of the GPR waves within the soil that may conceal the true response from the CS targets, also may affect the quality of the radargrams. The feature of interest in the radargrams were the CS hyperbolic responses, which in this research were deficiently weak, tainted by noise, and, in some cases, they were not visible. The intuitive analysis of the radargrams was not possible due to the complexity of the data. The Fast Discrete Curvelet Transform (FDCT), an image processing technique, was applied accordingly to discriminate CS from surrounding noise (i.e., increase the signal-to-noise ratio - *SNR*). Discrimination was an essential aspect in CS detection. The horizontal features or antenna ringing, and clutter responses were reduced on the radargrams and the FDCT was used to emphasize the edges or curves of the hyperbolic seed responses. The process of discriminating and identifying CS hyperbolic responses was performed in a stepwise approach to suppress noise responses and simultaneously enhancing SNR of the subtle hyperbolic responses in the radargrams, and most importantly being heedful not to discard essential details within the image. The discrimination of CS was achieved by varying the scales and angles of the FDCT-Wrap method to attain the desired image quality (i.e., showing defined hyperbolas). The FDCT scales and angles were dependent on the input image.

How the FDCT works

The FDCT-Wrap algorithm is suited to images with edges or curves, whereby the coefficients are calculated to enhance curves in an image. For example, an input to the FDCT-Wrap is a Cartesian array *f (m, n)* of a 2D image with *M* by *N* dimensions. The array is then decomposed to digital Curvelet coefficients computed as shown in equation (1). The FDCT digital coefficients are indexed by the scale *j*, orientation *l*, and spatial location parameters k_1 and k_2 (AlZubi et al., 2011). From the estimated coefficients, the FDCT-Wrap selects Fourier samples for the reconstruction of the image and only the largest coefficients are used while small are discarded (set to zero) as they are subjugated by noise.

$$C^D(j,l,k_1,k_2) = \sum_{0\le n\le N}^{0\le m\le M} f[m,n]\varphi^D_{j,l,k_1,k_2}[m,n] \quad [3]$$

where φ^D_{j,l,k_1k_2}, is the digital Curvelet waveform, and D is for the digital. The matGPR is a software package that is used in MATLAB. The FDCT-Wrap technique is a built-in function of the matGPR developed by (Tzanis, 2006, 2013, 2015).

CS depth

CS planting depths were estimated using equation (4):

$$D_e = \frac{ct}{2\sqrt{\varepsilon}} \quad [4]$$

where D_e is the estimated CS depth (m), c is the speed of light (m ns^{-1}), t is the two-way time to target (ns), and ε is the relative dielectric permittivity. The matGPR has the capability to provide the CS coordinates (x, y) from the 2D image and an index representing the pixel intensity (apex amplitude). The x and y represent the spatial distance and total two-way travel time (depth), respectively. The relative dielectric permittivity was calculated using the Topp's dielectric and soil mixing models (Peplinski et al., 1995; Topp et al., 1980). The effects of the treatment factors of the two respective dielectric models were assumed to be factored by the models to minimize error in predicting the soil dielectric permittivity and the CS planting depth.

Moreover, a third model was introduced to calculate the dielectric permittivity of the two soils in the study. The dielectric model was developed as a function of the dielectric permittivity from the soil mixing *(M)* and Topp's dielectric *(T)* models as shown in equation (5). We termed the prediction model the *Topp-Mixing (TM)* model. The model purpose was to minimize and optimize planting depth error (PDE) by combining the effects of the treatment factors from *T* and *M*. Equation (6) represent a linear regression model with coefficients predicted as explained below:

$$y_i = \varepsilon_{TM} = f(M, T) \quad [5]$$

$$\varepsilon_{TM} = \alpha + \beta X_i + \epsilon_i = \beta_0 + \beta_1 M_i + \beta_2 T_i + \epsilon_i \quad [6]$$

where ε_{TM} is the *TM* dielectric permittivity, $\hat{\beta}_i$ model coefficients, ϵ_i is the model error. The expected mean model error is zero ($\epsilon_i = 0$).

The measured data was randomized and split into training and testing sets. The training set had 70% of the data points while 30% was reserved for testing. From the training data we predicted the linear regression coefficients $\hat{\beta}_i$. The algorithm that predicts the $\hat{\beta}_i$ search for the global minimum values of the training data to minimize the statistical difference in the predicted and actual depths. The $\hat{\beta}_i's$ were used to estimate the dielectric permittivity $\hat{\varepsilon}_{TM}$ from test data. The accuracy of the predicting coefficients were determined by comparing the training and testing adjusted sum of squared error (SSE), estimated as shown in equation (7):

$$SSE = \sum_{i=1}^{n} \left(y_i - \hat{y}_{i,-i}\right)^2 \quad [7]$$

where y_i is the actual depth measurement, $y_{i,-i}$ is the predicted depth measurement with leave-one-out, n sample size of the training data and i position of an element in the training data. The $\hat{\beta}_i$ values would be estimated in such a way that they minimize the SSE parameter. To achieve the latter, the cost function *J* was used as shown in equation (8):

$$\frac{dJ}{d\beta}\Big]_{min} = \frac{dSSE}{d\beta} = \frac{d\left(y_i - \frac{ct}{2\sqrt{\varepsilon_{TM}}}\right)}{d\beta} = \frac{d\left(y_i - \frac{ct}{2\sqrt{\beta_0 + \beta_1 M_i + \beta_2 T_i}}\right)}{d\beta} = 0 \quad [8]$$

Data analysis methods

The match and select algorithm was developed to match the measured seed spacing to the known spacing values. A parameter termed Coefficient of Precision (CP3) was used. The CP3 parameter assesses the seed spacing uniformity by accounting for variation spacing in a row. The parameter has been reported to have different tolerances depending on the planter seeding delivery and correlated to the forward speed and field slope (Kocher et al., 2011; Searle et al., 2008). The greater the percentage spacing (e.g., > 70%) would be considered good, while the others e.g., < 70% would have more variations in spacing or inconsistent. Therefore, the CP3 is the percentage of seed spacing that falls within the ±1.5 cm of the theoretical spacing. The tolerance adopted for our laboratory experiment was ±3 cm (1.2 in.) of the CS spacing. The idea was during CS burial using levelers seeds may have shifted from their original positions; hence the tolerance. Also, for the assessment of the 2.6 GHz antenna effectiveness and accuracy to measure CS depth, the coefficient of planting depth accuracy (CPDA) was used. For our experiment, ±0.5 cm of the theoretical planting depths was used as the CPDA. The CPDA value represent the percentage value that deviates from the theoretical measurement that is within the ±0.5. Lower percentage values of the CPDA would represent the lowest minimal deviation from the recommended theoretical planting depths.

Results

The raw radargrams in figure 3 collected are presented as measured, from sandy-loam and loam soils at the three VMC groups. The data was profoundly noisy with 500 sample x 1024 traces with a sample rate of ~ 0.0024 ns (time window of 2.5 ns) and trace spacing of 0.3048 cm (section length of 152.4 cm). The most important characteristic in the images were

the signatures of the buried CS. In the figure 3, the CS hyperbolic signatures are not all visible on the radargrams due to clutter or soil inhomogeneity. Also, as observed on the radargrams, there are dominant antenna ringing (horizontal features), which shadowed details or obscured the CS hyperbolic responses. The presence of the hyperbolic responses at the location where seeds were placed indicated detection of the CS in the soil.

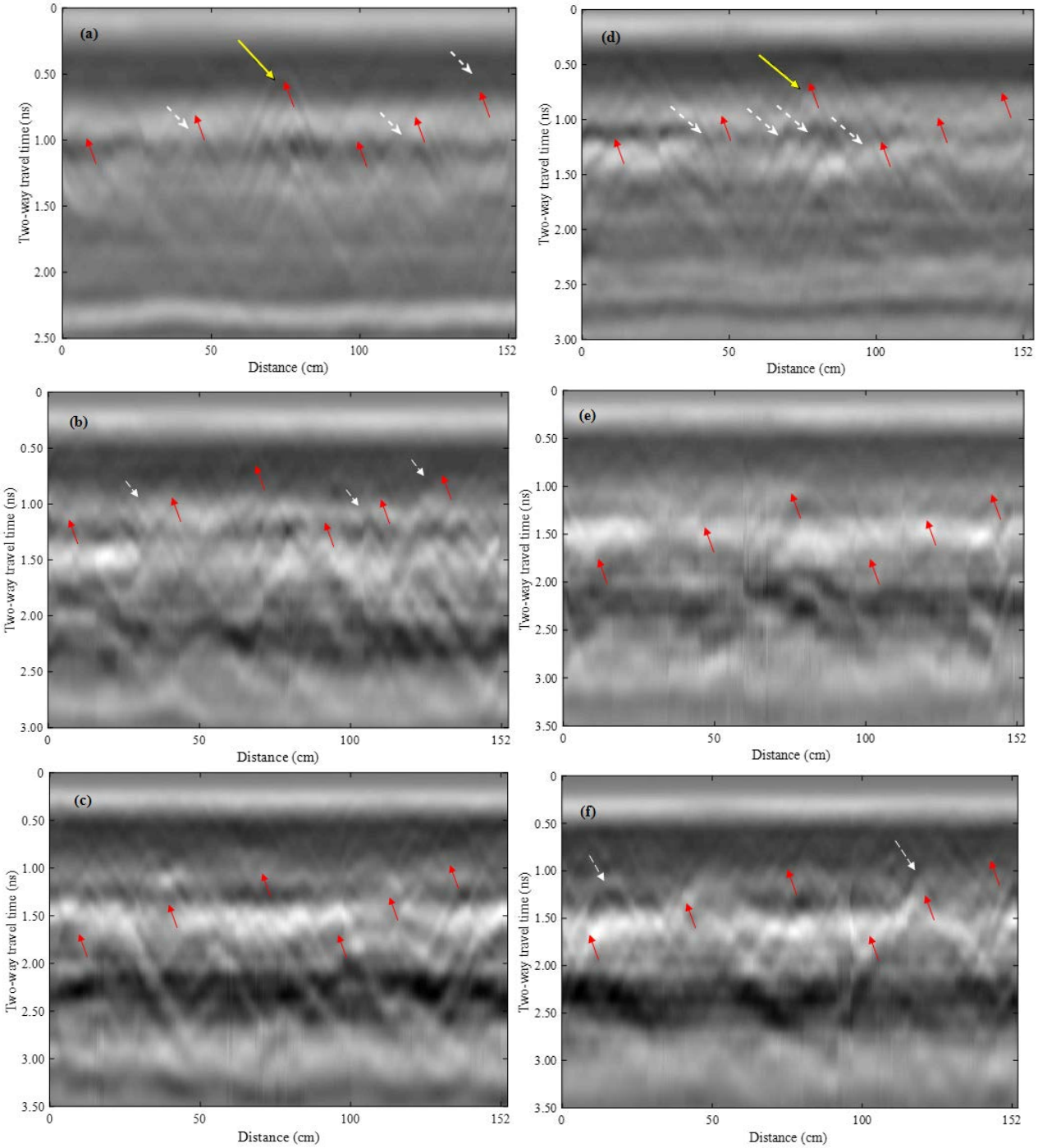

Figure 3. GPR raw data of buried CS in sandy-loam and loam soils, (a, b, and c) represent radargrams from dry, intermediate, and moist sandy-loam, and (d, e, and f) represent radargrams that were collected from dry, intermediate, and moist loam. The red arrows show the positions where CS should be in the image. The yellow arrows show the identified CS with faded hyperbolas. The white arrows show positions of the undetected CS (no hyperboles) or undiscernible responses or the responses that are either from CS or artefacts within the soil.

In the dry group (top 2 images), the two soils surrounding the CS were deficient in moisture contents compared to the CS. This phenomenon created a substantial dielectric contrast between the soil and CS. Because of the dielectric contrast in moisture, the CS were successfully located at different depths and spacing. However, not all CS were detected, and some seeds showed extremely faded hyperbolic responses and others that were not substantively perceptible. Also, observed in the dry category was the decrease of the antenna gradient to map the CS that were buried deeper in the soil bins. Near-surface CS (3.81 cm) were evidently distinguished from soil matrix compared to the CS that were buried deeper (8.89 cm). For the replicates collected, deeper CS were hardly visible and in some cases were observed to show no response (fig 3a&d).

For the figures with no yellow arrows, it was difficult to identify CS visually. The radargrams showed different total two-way travel times depending on the soil VMC group. For instance, the drier soils showed less two-way travel time compared to wet soils.

In the intermediate (middle 2 images), and moist categories (bottom 2 images), CS were sparsely detected. The two soil VMC groups were observed to affect the CS detection profoundly. Multiple intermittent reflections at the location and regions around the CS and strong horizontal ringing within the radargrams were observed (noise variation due to artifacts, soil moisture). It was difficult to visualize where the target were within the radargrams. For the intermediate group, it made sense when CS were not detected – the sandy-loam and loam VMCs were proximal to CS moisture; therefore, they were little or no contrasting interfacial properties between the soils and CS. Therefore, no reflection led to the suggestion that the 2.6 GHz antenna was seeing a single layer along the GPR wave propagation path. However, it could have made sense at the moist group to have detected CS because of the disparity in the two moistures between soil and CS. The moist soils had higher VMC which confounded the detection of the CS. The confounding effect had reduced the antenna resolution (see vertical and horizontal resolution) to map buried CS in some specific (higher moisture conditions) spatial domain characterized by sparse mapping figure 3(b, c, and e, f). Nonetheless, the Fast Discrete Curvelet Transform image processing technique was used to denoise and discriminate CS from artifacts, and clutter scattering.

GPR image processing using Fast Discrete Curvelet Transform (FDCT)

Collected radargrams predominantly convey the positions of the buried CS. For some of the radargrams the CS positions were not visible within the image because the images were heavily subjugated by noise, particularly in intermediate and moist VMC groups (see fig. 3(b, c, and e, f). Therefore, image enhancement was necessary for the CS position accentuation, to enable the GPR data analysis and interpretation. Firstly, we explored the concept referred to as the background subtraction (BGR). For the BGR, a difference of the CS and averaged target-free A-scan was calculated the result is shown in figure 4. Figure 4, illustrates an A-scan before and after background subtraction. Accordingly, the BGR was substantially efficient for CS that had partially strong hyperbolic responses, figure 3a (*marked with yellow arrow*). The parameters such as the amplitude and two-way travel time were extracted from the figure. It was observed (fig. 4) that the CS amplitude was normalized to the baseline. The estimated CS two-way travel time was 0.59 ns with amplitude of 2216 after BGR. After zero-correction time was performed, the buried CS depth was predicted to be 3.68, 4.78, and 4.85 cm from the Topp-Mixing, soil mixing model, and Topp's dielectric model, respectively.

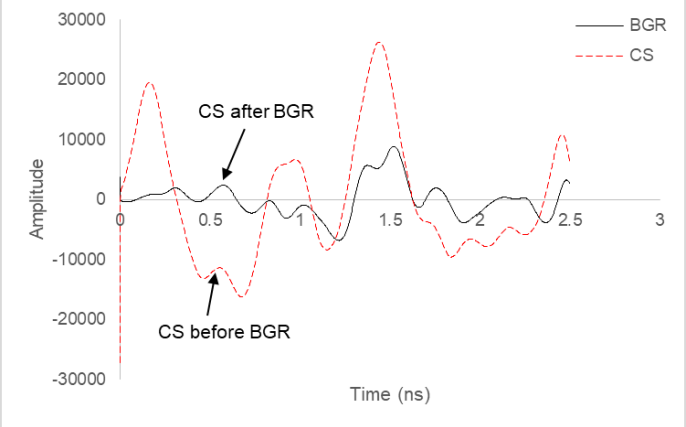

Figure 4. A-scan background subtraction.

The BGR would have been suitable for all CS buried at different depths in the soil-bin and with discernible hyperbolas. The BGR method, however, is point-based and localized. The disadvantage with this point-based technique is that the image cannot be reconstructed, and the selected window width does not always work on targets that are buried at different depths having deficient amplitude intensity. The results have shown that (even though soils were clean) there were high soil inhomogeneities that contaminated the data and perhaps distorted CS responses. The lack of the soil uniformity resulted in the BGR process not being used.

The FDCT-Wrap technique was capable of subduing noisy elements and enhance the hyperbolic responses through suppression of ringing noises, and enhancement of the curve edges from the Curvelet waveform coefficients. The estimated Curvelet waveform coefficients can only work to a certain extent to denoise and enhance the curve singularities on the B-scan. For instance, fairly weak hyperbolic responses (fig. 5a) were successfully improved by the Curvelet waveform coefficients (fig. 5b). Even after applying the FDCT-Wrap technique, in some radargrams CS responses were not visible. However, due to the complexity of the radargram, the technique was capable of improving the edges or curves that were thought to have come from artefacts or constructive interferences (ghost hyperboles). Coincidentally, some of these strong edge response (artefact responses) occurred at the locations where the CS should have been and some everywhere else within the picture as shown in figure 5c.

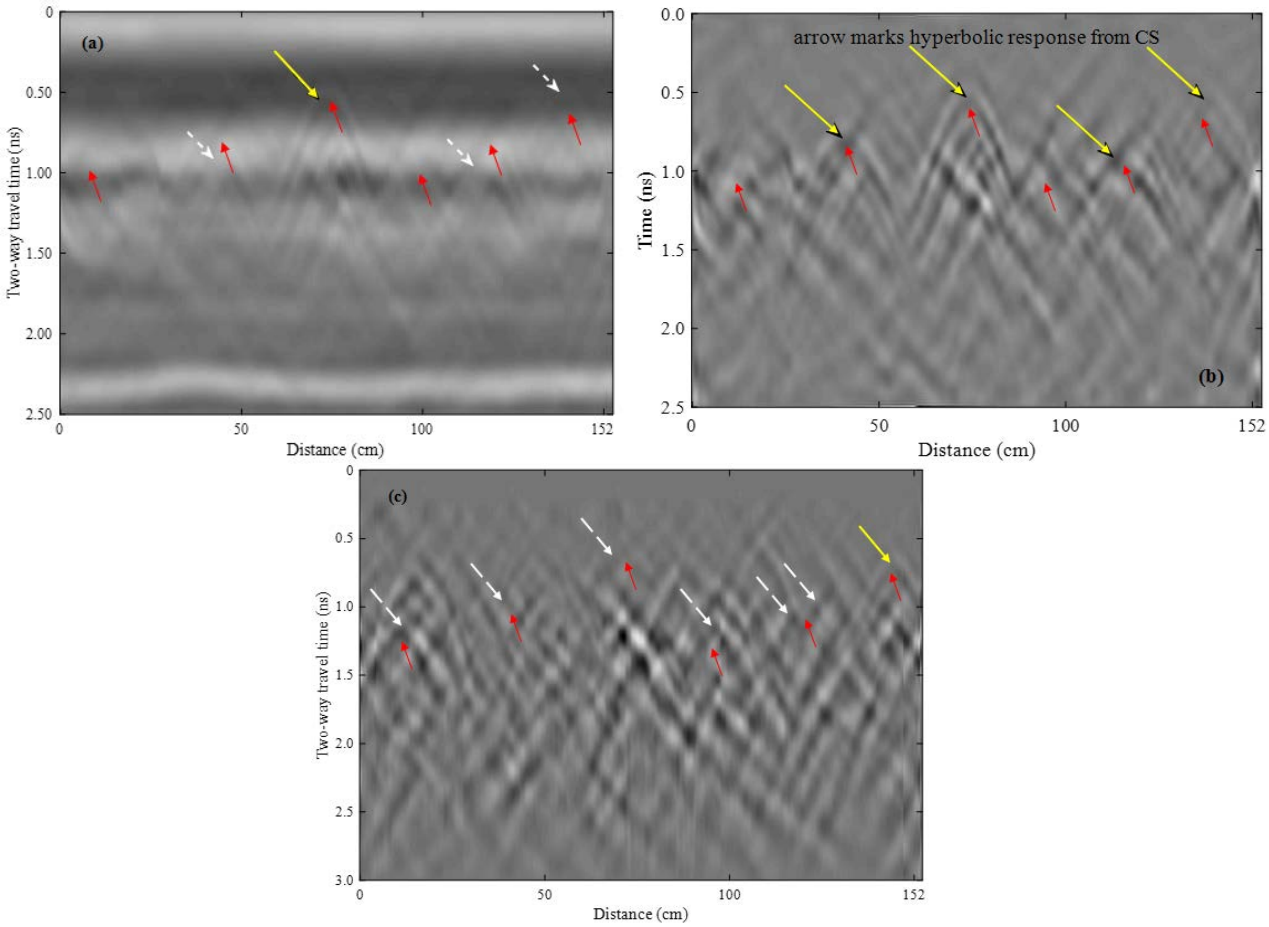

Figure 5. Radargrams collected from the sandy-loam soil: (a) raw radargram from dry VMC group with one target visible, (b) processed radargram from dry VMC group with few CS targets visible, and (c) processed radargram from intermediate VMC group with mostly strong edges from artefacts. The red arrows show the locations where CS are supposed to be and the yellow arrows show identified or visible CS hyperbolic responses. The white arrows indicate un/discernible responses that are either from CS or artefact within the soil.

Extracting the important parameter (two-way travel time) from figure 5c was complicated. Consequently, for these kind of data (fig. 5c) we proposed that (1) for any surrounding hyperbolic response that was proximal to temporal spacing and depth positions of the CS within the image, their parameters were extracted and (2) a matching and selecting algorithm was developed to match the temporal spacing and depth positions of the hyperbolic response to the actual spacing and depth as discussed in the methodology section. The matching and selecting algorithm used the CP3 and CPDA values of ±3 cm and ±1.0 cm, respectively and few data points were obtained. The GPR CP3 values for the CS spaced 25.4 cm apart were 28%, 24%, and 26% in dry, intermediate, moist groups, respectively were detected. For the CS spaced 15.24 cm the CP3 values were 15%, 7%, and 20% in dry, intermediate, moist groups, respectively were detected (table 5). These numbers are typical low for CP3. The disparity in the spacing precision was primarily from inability of the 2.6 GHz GPR antenna to actually detect seeds in sandy-loam and loam soils in different moisture groups. The CS that were detected out of the total CS used in the experiment replications were extremely low in quantity hence the low values of the CP3.

Statistical analysis

Estimation of the Topp-Mixing model

From the experimental data, the following linear regression model coefficients were estimated: $\beta_0 = 4.90, \beta_1 = 0.64, and\ \beta_2 = -0.48$ with p-values of $p_0 = 1.58e-10, p_1 = 0.19, and\ p_2 = 0.39$. The predicted *TM* model is given in equation (9);

$$\varepsilon_{TM} = 4.90 + 0.64M_i - 0.48T_i + \epsilon_i \quad [9]$$

The most important factor in mapping CS was to accurately estimate the CS spacing and planting depths using GPR. The measured spacing and depths (table 4) were compared to the known CS spacing and depths by determining the sums of squared error (SSE) statistics. The predicted SSE statistics for the Top-Mixing, soil mixing, and Topps dielectric models were 17.93, 30.53, and 31.82, respectively. The Topp-Mixing model had the lowest SSE statistics which showed that the predictive ability of the model was efficient in estimating the dielectric permittivity of the soil. In table 4 we show average measured spacing and depth measurements and standard deviations associated with each measurement model.

Table 4. Descriptive statistics comparison of GPR estimated CS depth in dry sandy-loam and loam soils according to the CS spacing

Dielectric model	Actual depth (cm)	15.24 cm CS spacing	25.4 cm CS spacing
Soil mixing dielectric model	3.81	4.32 (1.04)	4.57 (1.09)
	6.35	6.10 (1.52)	7.11 (1.35)
	8.89	8.13 (1.35)	8.38 (1.17)
Topps dielectric model	3.81	4.57 (1.12)	4.83 (1.17)
	6.35	6.10 (1.52)	7.37 (1.40)
	8.89	8.38 (1.14)	8.64 (1.17)
Topp-Mixing dielectric model	3.81	4.32 (0.69)	4.57 (0.99)
	6.35	5.842 (0.94)	6.60 (1.12)
	8.89	7.87 (0.66)	8.64 (0.9144)

Table 5. Estimated CP3 value from the 2.6 GHz antenna per soil VMC group

CS spacing (cm)	Dry (%)	Intermediate (%)	Moist (%)
15.24	15.00	7.00	20.00
25.40	28.00	24.00	26.00

Table 6. Analysis of variance on the effect of each treatment factor in the prediction of CS planting depth based on the three dielectric models.

Source	DF	Topp-Mixing model F Ration (Prob > F)	Soil mixing model F Ration (Prob > F)	Topp's model F Ration (Prob > F)
Soil	1	2.42 (0.1229)	3.66 (0.0585)	0.78 (0.3799)
VMC group	2	0.10 (0.9032)	20.37 (2.657e-08)	17..08 (4.183e-07)
Soil : VMC group	2	7.03 (0.0014)	8.15 (0.0005)	9.08 (0.0002)
Error	5			

Table 7. Least Square Means with standard error for the CPDA parameter for all combination of the treatment factors: soil, VMC group and the interaction of the soils and VMC groups

CS depth estimation model	Least Square Means	Standard error
Topp's dielectric (%)	22.42	3.37
Soil mixing (%)	18.82	3.14
Topp-Mixing (%)	9.94	2.58

The Analysis of variance (ANOVA) was performed on the measured CS depth to establish the treatment factors that were significant (Table 6). To determine the significant difference between the treatment factors (soil and VMC group and the soil-VMC group interaction) the test was executed at a 0.05 level of significance using R. The ANOVA indicates there is a significant interaction between the soil and VMC group across the three covariate models. The soil across all the depth models was not significant and the VMC group was not significant for the Topp-Mixing model.

The effect of each treatment factor in the predictive models was evaluated on the CPDA parameter. The Least Square Means with standard error are presented in Table 7 and the calculation of least square means were based on the percentage CPDA. The three models show the marginal means of the predicted CPDA for CS planting depth. The Topp-Mixing, soil mixing, and Topp dielectric model had 9.94%, 19.82%, and 22.42%, respectively. The Topp dielectric model was performing badly in the prediction of depths (higher CPDA) while the Topp-Mixing model was determined to be the best model to predict the depths (lower CPDA).

Discussion

The purpose of this study was to introduce a new method of estimating CS planting depth and spacing in a non-destructive manner. Measuring CS spacing and depths non-destructively is vital and would prevent utilization of the destructive method (*conventional method – dig and search*). Non-destructive measurements may reduce error in measurements and repeatability in measurements would be possible compared to destructive method. A complete randomized design was implemented. The utility of 2.6 GHz GPR antenna to detect and quantify CS planting depth was evaluated in soil bins under controlled laboratory conditions and met with infrequent success. The radargrams acquired were meager with prevalent noise. The major finding of our study were that the dry soils and water contents of the buried CS were critical in the detection. Though moisture confounds GPR wave detection, it is evidently shown in this study that CS moisture content played an integral part in GPR application for locating buried CS in drier soils (fig. 5a). For subsurface detection a sufficient gradient between soil and roots has to exist (Bain et al., 2017), which was observed to be the case in this particular study for CS. Furthermore,

results suggest that GPR at the right frequency and appropriate soil VMC, it can be a tool for quantifying seeds in future research.

Although the radar waves were capable to penetrate the soil beyond 17.78 cm in the soil bins at intermediate and moist groups, it was difficult to detect CS. The dispersion of the wave within the soil may have been great to obscure the CS responses. One thing to note was the CS used in the study were small in size (PDR size) and their orientation layout in the soil bins did not have an effect in detection. The extraction of the CS responses using GPR was difficult in processed soils. Though the soils were processed a number of limiting factors may have hid or distorted CS responses. During data processing the following points were made as probable limiting factors for the GPR detection: 1) effects from the antenna frequency whereby multiple intermittent scattering were prevalent; 2) the soil physical properties that governed GPR wave velocity, attenuation, absorption; 3) the dielectric contrast between the soil and the CS determining the strength of the CS response and; 4) the CS size and the shallow depths. The ineffectiveness of the 2.6 GHz GPR was correlated with higher soil VMC and somewhat the CS size and shallow depths. The prevalence of multiple intermittent scattering at higher soil VMC was overwhelming hence the radargrams quality were sub-par with no discernible CS responses.

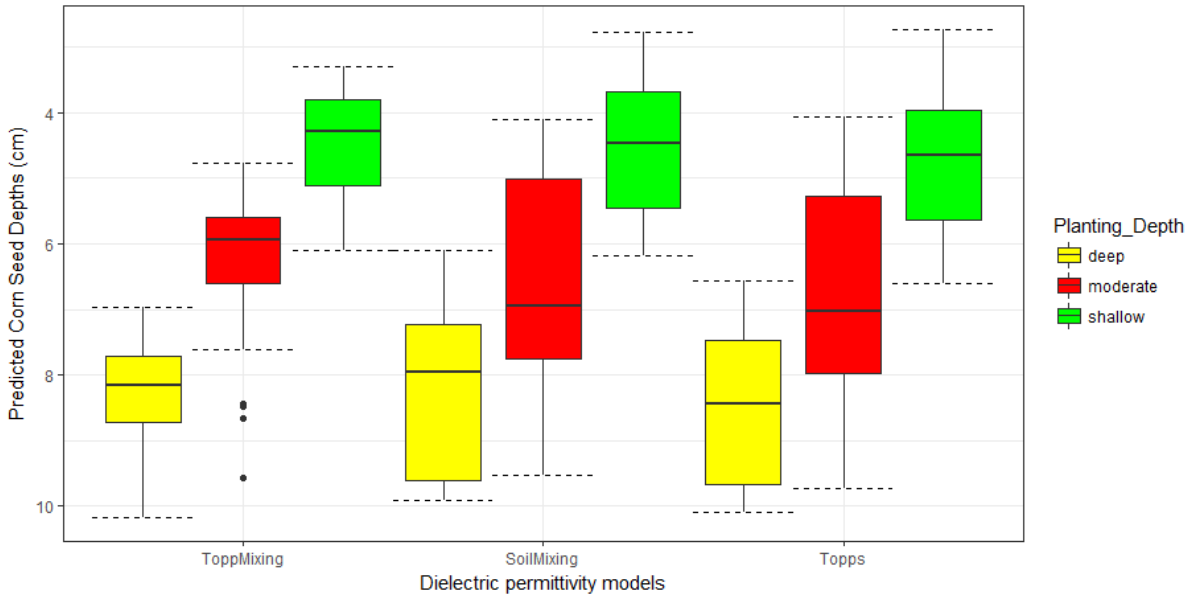

Figure 6. Boxplots for temporal CS depths estimated using three dielectric permittivity models. Planting depth: shallow, moderate, and deep correspond to 3.81 cm, 6.35 cm, and 8.89 cm, respectively. (*ToppMixing = Topp-Mixing model, SoilMixing = Soil mixing model and Topps = Topp's dielectric model*).

The three models were compared based on the CPDA value. The dielectric permittivity estimated using the Topp-Mixing, Topps dielectric and soil mixing models were in some cases underestimating or overestimating the planting depth (table 4) which may have been influenced by several covariates and confounding factors. The statistical analysis indicates the significant of the interaction between the soil and VMC groups. This may mean the amount of water in the soil was critical in the detection of seeds (as explained above). The boxplots in figure 6, show the distribution of the predicted planting depths based on the three predictive models. The Topp-Mixing model displays a narrow distribution of the three depths measured with an exception of the outliers at the 6.35 cm. The narrow distribution could mean most of the predicted depth measurements were proximal to the known depths (3.81 cm, 6.35 cm, and 8.89 cm). While the soil mixing and Topp dielectric models were predicting close to the mean depths, the distribution of the measured depths was spread out.

The objectives of this research were successfully met when soils were dry, however, this moisture deficient soil condition is not conducive for CS planted to germinate. More research needs to be conducted with different sets of GPR frequencies higher than the 2.6 GHz used in this study or combination of other sensing mechanisms in tandem to increase chances of mapping seeds in a variety of soil conditions. The preliminary results presented in this study showed a positive development towards the attainment of a non-destructive technique to map CS spacing and planting depth. We recommended further studies with different CS variety, and soils to evaluate the GPR and progression of this work.

Conclusion

Experiments were performed to detect CS using 2.6 GHz Ground Penetrating Radar (GPR) in two soils: sandy-loam and loam with different conditions. The two parameters: CS spacing, and depth were quantified with mixed success. The CS were buried at three different depths and two different spacing. The soil VMC were divided into three groups; dry, intermediate, and moist of which were within 2.31% to 17.07% for the sandy-loam and 2.50% to 18.80%, for the loam. Pioneer P0339AMXT of seed size PDR (1459 kernels/lb.) corn variety were used with determined moisture of 10.05%

(d.b.). The primary objective of the study was met. In conclusion, the main findings of this investigative study were: (i) the developed Topp-Mixing model from the experimental data yielded best CPDA compared to the soil mixing and Topps dielectric model. The models, however, there were instances where they underestimated or overestimated CS spacing and planting depth, and (ii) the preliminary results in this research indicates that the 2.6 GHz GPR antenna can quantify CS planting depth and spacing within an accuracy of 10%. In addition, CS were mostly detected in drier soils (dry moisture group), however, more research is needed to enable detection of CS in soil conditions that are typical during planting operations in fields.

References

AlZubi, S., Islam, N., & Abbod, M. (2011). Multiresolution analysis using wavelet, ridgelet, and curvelet transforms for medical image segmentation. *Journal of Biomedical Imaging, 2011*, 4.

Andrade, F. H., & Abbate, P. E. (2005). Response of maize and soybean to variability in stand uniformity. *Agronomy Journal, 97*(4), 1263-1269.

Andrews, W. F. (1981). *Soil survey of Boone County, Iowa*: US Department of Agriculture, Soil Conservation Service.

ASTM. (1972). Standard Method of Laboratory Determination Of Moisture Content of Soil. In *D2216-71*. American National Standards Institute.

ASTM. (2018). Standard Test Methods for Laboratory Determination of Density (Unit Weight) of Soil Specimen[1]. In *D7263-09*. American Society for Testing and Materials.

Bain, J. C., Day, F. P., & Butnor, J. R. (2017). Experimental Evaluation of Several Key Factors Affecting Root Biomass Estimation by 1500 MHz Ground-Penetrating Radar. *Remote Sensing, 9*(12), 1337.

Barton, C. V., & Montagu, K. D. (2004). Detection of tree roots and determination of root diameters by ground penetrating radar under optimal conditions. *Tree physiology, 24*(12), 1323-1331.

Beck, S. (2014). *Practical Farm Research (PFR)*. Atlanta: Beck's Hybrids.

Butnor, J. R., Doolittle, J., Johnsen, K. H., Samuelson, L., Stokes, T., & Kress, L. (2003). Utility of ground-penetrating radar as a root biomass survey tool in forest systems. *Soil Science Society of America Journal, 67*(5), 1607-1615.

Butnor, J. R., Doolittle, J., Kress, L., Cohen, S., & Johnsen, K. H. (2001). Use of ground-penetrating radar to study tree roots in the southeastern United States. *Tree Physiology, 21*(17), 1269-1278.

Cui, X., Guo, L., Chen, J., Chen, X., & Zhu, X. (2013). Estimating tree-root biomass in different depths using ground-penetrating radar: evidence from a controlled experiment. *IEEE Transactions on Geoscience and Remote Sensing, 51*(6), 3410-3423.

Dannoura, M., Hirano, Y., Igarashi, T., Ishii, M., Aono, K., Yamase, K., & Kanazawa, Y. (2008). Detection of Cryptomeria japonica roots with ground penetrating radar. *Plant Biosystems, 142*(2), 375-380.

Doerge, T., Jeschke, M., & Carter, P. (2015). Planting Outcome Effects on Corn Yield. *Crop Insights, 25*(1), 1-7.

Hussen, S., Alemu, B., & Ahmed, F. (2013). Effect of Planting Depth on Growth Performance of Maize (Zea-Mays) at the Experimental Site of Wollo University, Dessie, Ethopia. *International Journal of Sciences: Basic and Applied Research (IJSBAR), 8*(1), 10 - 15.

Kocher, M. F., Coleman, J. M., Smith, J. A., & Kachman, S. D. (2011). Corn seed spacing uniformity as affected by seed tube condition.

Koller, A. A., Wan, Y., Miller, E. A., Weckler, P. R., & Taylor, R. K. (2014). Test method for precision seed singulation systems. *Transactions of the ASABE, 57*(5), 1283-1290.

Liu, W., Tollenaar, M., Stewart, G., & Deen, W. (2004). Response of corn grain yield to spatial and temporal variability in emergence. *Crop Science, 44*(3), 847-854.

Mapoka, K. O., Birrell, S. J., & Tekeste, M. (2016). *Modeling Ground Penetrating Radar (GPR) Technology for Seed Planting Depth Detection using Numerical Scheme based on Finite Difference Time Domain (FDTD) Method*. Paper presented at the 2016 ASABE Annual International Meeting.

Nelson, O. S. (2005). Dielectric Properties Measurement for Agricultural Applications. doi:10.13031/2013.19107

Peplinski, N. R., Ulaby, F. T., & Dobson, M. C. (1995). Dielectric properties of soils in the 0.3-1.3-GHz range. *IEEE Transactions on Geoscience and Remote Sensing, 33*(3), 803-807. doi:10.1109/36.387598

Pérez-Gracia, V., González-Drigo, R., & Di Capua, D. (2008). Horizontal resolution in a non-destructive shallow GPR survey: An experimental evaluation. *NDT & E International, 41*(8), 611-620.

Raper, R. L., Asmussen, L., & Powell, J. B. (1990). Sensing hard pan depth with ground-penetrating radar. *Transactions of the ASAE, 33*(1), 41-46.

Rial, F. I., Pereira, M., Lorenzo, H., Arias, P., & Novo, A. (2009). Resolution of GPR bowtie antennas: An experimental approach. *Journal of Applied Geophysics, 67*(4), 367-373.

Searle, C. L., Kocher, M. F., Smith, J. A., & Blankenship, E. E. (2008). Field slope effects on uniformity of corn seed spacing for three precision planter metering systems. *Applied Engineering in Agriculture, 24*(5), 581-586.

Test, P.-p. S. N. (1998). Nitrate-nitrogen. *Recommended Chemical Soil Test Procedures*, 17.

Topp, G., Davis, J., & Annan, A. P. (1980). Electromagnetic determination of soil water content: Measurements in coaxial

transmission lines. *Water resources research*, *16*(3), 574-582.
Tzanis, A. (2006). *MATGPR: A freeware MATLAB package for the analysis of common-offset GPR data*.
Tzanis, A. (2013). Detection and extraction of orientation-and-scale-dependent information from two-dimensional GPR data with tuneable directional wavelet filters. *Journal of Applied Geophysics*, *89*, 48-67.
Tzanis, A. (2015). The Curvelet Transform in the analysis of 2-D GPR data: Signal enhancement and extraction of orientation-and-scale-dependent information. *Journal of Applied Geophysics*, *115*, 145-170. doi:https://doi.org/10.1016/j.jappgeo.2015.02.015